5
Voltage Induced Molecular Motors Constitute the Smallest Self-Assembled Molecular Electronic Counter: An experimental Study of Molecular Device

In this chapter the study revolves around the experimental realization of molecular devices at atomic scale in a scanning tunneling microscope (STM) in ultra-high vacuum (UHV) conditions. In the previous chapter a single molecule, 2,3-Dichloro-5,6-dicyano-1,4-benzoquinone (DDQ), device was studied with the help of DFT method. In this chapter the same DDQ molecule was deposited on gold surface under UHV conditions by e-beam evaporator and processed under sputtering system to remove residual particles to finally characterize with the help of STM system. The IV results obtained by this study on single DDQ molecule coincide with that of obtained from theoretical study in the previous chapter. And thus, this study confirms the electrical properties of single molecule at atomic scale. This study also illustrates how self-assembly of DDQ molecules may work as an electronic counter.

5.1 Introduction

The miniaturization of conventional electronic components brings the electronic industry to the brink of the threshold of reduction after which the components cannot work efficiently (Keyes, 2000; Kish, 2002; Wong and Iwai, 2005). One of the biggest challenges of the computing world is to fit a higher number of transistors into a microchip to increase the speed of computation (Geist and Lucas, 2009; Peercy, 2000). These transistors occupy limited space in the chip and as predicted by Gordon Moore the size of the transistors have shrunk to the extent that the number of these transistors in the chip has almost doubled roughly in every two years (Moore, 1965). The shrinking size of the transistor leads to issues such as non-reliable performance of the devices, overheating due to extensive contact resistances (Kish, 2004; Pop et al., 2006), and increase of leakage current (Agarwal et al., 2006) to name some of them. An alternate method to circumvent the problems is to follow the slow but efficient natural computing method, which is being followed by all the living organisms. The benefit is that the scale of computation is massive, but it is impossible to achieve this with the traditional methods. One of the closest approaches to the natural computing process is to use synthetic molecules which are primarily consisting of carbon atoms and replicate the physical phenomena by using a self-assembled structure where the molecules will be allowed to interact with each other till they reach the minimum energy configuration.

Some of the well-known molecules which can be potentially used for this purpose are DRQ, Rose Bengal, DDQ. The common structural and functional attributes of these molecules are their redox behavior owing to the presence of some redox active groups (Bandyopadhyay and Miki, 2008; Bandyopadhyay and Pal, 2003b; Mukherjee et al., 2007), which alleviate the impossibility of using these molecules for large scale computation. Moreover, these molecules have multiple conformational states (Bandhopadhyay and Pal, 2003) with each state having different conductance, which will be useful for assigning different logic states in a group of self-assembled molecules. So, achieving a self-assembled structure for these molecules, one needs the perfect condition for the molecules to come together. Usually, self-assembly is a process to

minimize the surface energy of the system (Whitesides and Grzybowski, 2002). There are multiple reports of achieving self-assembly of organic molecules in a scanning tunneling microscope (STM) (De Feyter and De Schryver, 2003; Dhirani et al., 1996; Kühnle et al., 2002; Poirier and Tarlov, 1995; Tao et al., 1993; Wan, 2006; Yang and Wang, 2009), but the application of these self-assembled structures is limited (Andres et al., 1996; Dorogi et al., 1995; Gao and Gao, 2010). In an Ultra-High Vacuum (UHV) STM, single molecules have been observed routinely and are manipulated using various techniques. They have been studied as molecular motors by the application of an external stimulus such as electric field (Seldenthuis et al., 2010; Tierney et al., 2011), optical signal (Augulis et al., 2009; Browne and Feringa, 2009; Pathem et al., 2013; Russew and Hecht, 2010; Saywell et al., 2016), mechanical forces (Ariga et al., 2011; Ariga et al., 2018; Hla et al., 2001; Kay et al., 2007; Ladenthin et al., 2016; Pawlak et al., 2012; Perera et al., 2013), etc. One such exciting process is the change in conformation/orientation of the molecule by applying a different bias voltage to the molecule (Alemani et al., 2006; Blum et al., 2005; Donhauser et al., 2001; Troisi and Ratner, 2002). The molecule may or may not change its conformation but may undergo a translational or rotational motion on the substrate (Shirai et al., 2005)(Kudernac et al., 2011; Stipe et al., 1998). This motion may follow a random walk on the surface by following the gradient of the energy on the surface. Such movement by a group of molecules is limited by the degrees of freedom of the group of molecules (Kwon et al., 2005), but when such movement happens on the surface, it may reveal the purpose of such consorted action. There is hardly any report on a single molecule or a group of molecules being used as an electronic component or a device for any kind of computing purpose except the work of Bandyopadhyay et al. which used a group of molecules on an Au {111} surface to solve some hard problems such as the growth of cancer cells, but it considered the molecule's different conformational states due to different voltage bias in association with interaction with the neighbors (Bandyopadhyay et al., 2010).

In this work, we have shown that DDQ molecule can be used as a flip-flop and the molecules self-assemble on an Au substrate in such a way that a group of four molecules forms a 4-bit electronic counter. Such counters are present throughout the surface and are shown to convert analog signal to digital signal. This conversion process need not be involving only four-bit counters, but a much complex network of flip-flops leads to a formation of the n-bit counter, and hence one can convert an analog signal to an ultra-digital signal at a much faster rate. Thus, this work perhaps takes us a bit closer to the reality of natural computing.

5.2 Experimental

5.2.1 Deposition of Au on mica surface

For the growth of an Au {111} on the mica surface, we have used standard protocol (Chidsey et al., 1988). Freshly cleaved muscovite mica substrates were kept in a vacuum oven at 200°C for 12 hrs and are used immediately. The Au {111} on a freshly cleaved muscovite mica surface was deposited by using thermal evaporation method at a pressure of 10^{-6} Torr. The rate of deposition was controlled at 0.1 nm/s and was continued till a 150 nm thick Au layer is deposited on the mica surface. While depositing the substrate temperature was maintained at 300°C. After the deposition, also the substrate was kept at 300°C for 1 hr and then slowly cooled down to room temperature. So, we can achieve an Au {111} reconstructed surface on mica which will be utilized for further application.

5.2.2 Deposition of DDQ on Au/mica surface

The as-deposited Au {111} on mica surface was first annealed and degassed at 500°C for surface reconstruction. Once the 22 x √3 reconstruction of Au atoms was achieved, the DDQ molecule was deposited. The deposition was carried out using e-beam evaporation method attached to the preparatory chamber of Omicron LT-STM. Molybdenum crucible was used for the deposition purpose, it is first degassed at 2A filament current, and 950V applied bias by bringing the crucible near to the filament. As crucible starts approaching filament, emission starts

increasing because of the electron beam. Crucible is degassed at emission current as high as 60.7 mA with a flux current of the order of 10^{-9}A and chamber pressure of the order of $1.6x10^{-7}$ mbar. DDQ molecule purchased from Sigma Aldrich was loaded into the crucible without further purification. Before depositing material on the substrate, it is first sublimated to remove any moisture. To ensure that no material evaporates into the chamber the evaporator is attached with a shutter shield. After sublimation of the material, it was ready for deposition on the substrate. For the deposition of the material applied voltage between crucible and filament was kept at 250V and filament current was set to 1.97A. The crucible was then approached to filament with very fine movement while keeping a constant eye on emission current, flux current, and chamber pressure. After e-beam formation, as observed by emission current, the rate of deposition was controlled by changing applied bias and the deposition lasted for 5 minutes. DDQ was deposited on the Au {111} surface. After deposition of DDQ, the substrate has undergone sputtering to remove residual DDQ clusters.

The images were taken in ultra-high vacuum and at room temperature using an Omicron LT-STM. An electrochemically etched Pt-Ir tip was prepared by following standard protocol (Libioulle et al., 1995) but with a little change in the recipe which is instead of using 20 V peak to peak we used a 13 V_{rms} with 50 Hz frequency till current value falls below 50 mA the tip prepared was used for the scanning of the DDQ deposited Au {111} surface in constant current mode. The Pt-Ir tip was placed over the substrate at a tunneling separation of 1-2 nm. The sample bias was -1V with a set current of 0.7nA. The whole experiment was performed in an Omicron LT STM, and the surface scanning was performed by using Omicron's Matrix software. The setup for the STM scan is shown in fig. 5.1(a).

5.3 Computational Methodology

We have calculated the charge density of different structures by performing first-principles calculations using the Vienna Ab-initio Simulation Package (VASP) (Kresse and Furthmüller, 1996). The Au $5d^{10}$ $6s^1$, C $2s^2$ and $2p^2$, Cl $3s^2$ and $3p^5$, N $2s^2$ and $2p^3$, O $2s^2$ and $2p^4$ electrons are considered as valence electrons. Plane waves with kinetic energies up to 400 eV are included in the expansion of the electronic wave function. The exchange-correlation energies are approximated using the generalized gradient approximation with the Perdew-Burke-Ernzerhof functionals (Perdew et al., 1996). The convergence criteria set for the electronic and ionic relaxation are 10^{-6} eV and 0.05 eV/Å, respectively. The Brillouin zone integration is performed on a Γ-centered 2×2×1 k-point mesh. Moreover, the Methfessel-Paxton smearing method is used with a smearing width of 0.01 eV (Methfessel and Paxton, 1989). So as to include any van der Waals interaction between the molecule and the substrate, the semi-empirical DFT-D3 method by Grimme et al. is employed (Grimme et al., 2010).

A supercell containing a mono-layer of Au(111) plane is constructed in such a way that the a-, b-, and c-axes of the supercell are oriented along the $[1\bar{1}0]$,$[11\bar{2}]$, and [111] directions in the Au-unit cell, respectively, and the monolayer is at the center of the supercell along the c-direction. The supercell lattice parameters are: a=11.753 Å, b=10.178 Å, and c=25 Å. A cell parameter of 25 Å along the c-direction results in a vacuum thickness of at least 17 Å between periodic images and ensures that there is no interaction between the periodic images. Two orientations of the DDQ molecule with respect to the Au (111) surface are considered in our study as shown in Fig. 5.1(b) and (c). The DDQ molecular plane normal is making an angle of 0°, and 30°with the Au (111) plane normal in configuration labelled (a) horizontal, (b) 30 degree, respectively. The DDQ molecule is placed above the Au (111) plane at a distance of approximately 3 Å and atoms are relaxed to the minimum energy positions. Charge density is calculated for the equilibrium configuration. Scanning tunneling microscopic (STM) images are generated from the charge densities employing the Tersoff-Hamann approach (Tersoff and Hamann, 1985; Vanpoucke and Brocks, 2008). Simulating the constant current mode by following a constant integrated local density of states as function of x,y and mapping z on a gray scale. Distance to the highest atom is set to 2.0 Å. Graphical smoothening of the calculated STM images is done

considering a tip radius of 1.25 Å to include the influence of tip geometry in the calculated images shown in fig. 5.1(d) and (e) (Vanpoucke, 2009). The corresponding experimental line profile are shown below each frame (d) and (e) which match with the theoretical line profile. When we compare both the experimental and theoretical topographic images, we can identify orientation of the individual functional groups of the molecule very easily.

5.4 Results and Discussions

Before depositing DDQ molecule, the gold surface was examined thoroughly. This is visible from the distinctive bright regions representing mainly the soliton waves (Fujita et al., 1997) sandwiching the darker region. The clean gold substrate shows the typical {111} crystal surface orientation where the compressed soliton lines sandwich the hcp region and are having fcc regions on to the left and right of them. The 22 x √3 arrangement of surface atoms is said to be due to the herringbone like reconstruction of the gold surface where a new atom is added after every 22 atoms along the $[1\bar{1}0]$ direction. The Au atoms are clearly seen in figure in all three figures of 5.1.

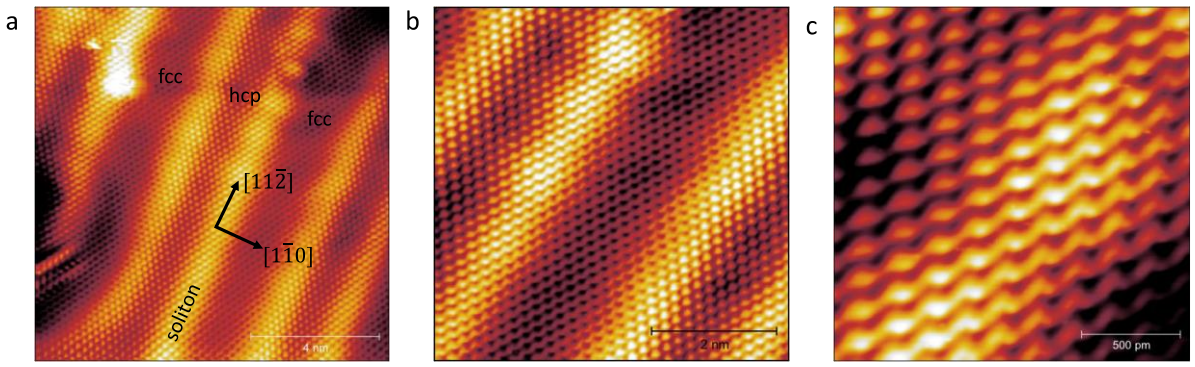

Fig. 5.1 (a) The Au {111} surface with herringbone on the surface. The two fcc layers are sandwiching the hcp layer to form the herringbone structure. The two ridges which represent the soliton waves have atoms arranged in two crystal planes as shown in the figure. The scale bar for the figure is 4 nm. (b) and (c) magnified images of the same surface with atomic resolution and the corresponding scale bars are 2 nm and 0.5 nm respectively.

The DDQ molecule that was used in our experiment has already been studied extensively to understand its electrical (Mukherjee et al., 2007; Mukherjee and Pal, 2005, 2006) and optical (Bandyopadhyay et al., 2006a) behavior. It has been known that DDQ is a redox active (Rath et al., 2008) molecule and has multiple oxidations and reductions potential. These potentials are attained by the change in the conformational state of the molecule (Grossel and Weston, 1994). The structure of the molecule is shown in fig. 5.2(f). The presence of oxygen atoms in the molecule helps in the reduction of the molecule owing to its high electronegativity. We tried to probe the single DDQ molecule electrically and studied the I-V curve shown in fig. 5.2(g). 80% of the time we got I-V curves which have NDR peaks in them and hence we chose to use the above I-V curve. The I-V curve has many peaks and valleys analogous to the negative differential resistance (NDR) effect. This feature has been explained based on contact resistance and the redox action of the molecule (Dagar et al., 2019). Though the I-V curve shows a flat region between -1.2 to 1.2 V, but the plot between absolute differential conductance with voltage shown in the inset of fig. 5.2(g) shows the actual behavior as it has its first peak in the negative bias at -1.15 V and in the positive bias at +0.86 V. These values correspond to the highest occupied molecular orbital (HOMO) level and the lowest unoccupied molecular orbital (LUMO) level of the molecule respectively as shown in fig. 5.2(h). The redox behavior of the molecule has been confirmed from the I-V curve as it matches with the theoretical observation.

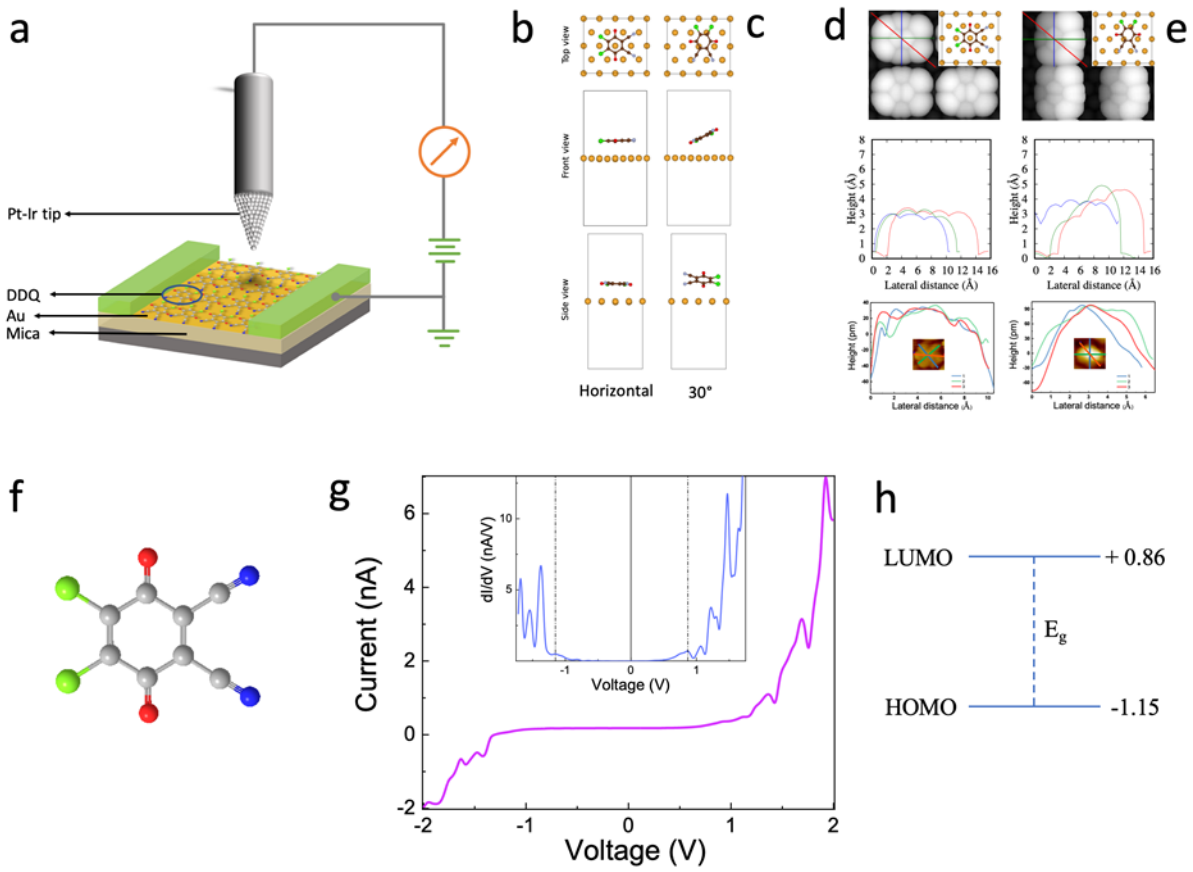

Fig. 5.2. (a) Schematic diagram of the scanning process in STM. The tip is at a tunneling separation from the substrate. The blue ellipse shows an individual molecule laying on the Au {111} substrate. (b) and (c) two orientations of the DDQ molecule on the Au (111) substrate: horizontal, and 30°, (d) and (e) simulated scanning tunneling microscope images of DDQ molecule on Au (111) monolayer in two configurations: horizontal, and 30°. The corresponding experimental line profile of the molecule is shown below each frame. (f) The stick and ball structural representation of DDQ molecule having carbon (C), nitrogen (N), oxygen (O), and chlorine (Cl) atoms represented by the grey, blue, red, and green balls respectively. (g) The experimental I-V characteristic curve measured from a single DDQ molecule within a voltage range of +2 to -2 V. The inset shows the absolute differential conductance plot obtained from the same molecule within the same voltage range in which the dotted lines correspond to the HOMO (left) and LUMO (right) energies. (h) The experimentally observed HOMO (-1.15 eV) and LUMO (+0.86 eV) energy levels of single DDQ molecule extracted from the differential conductance plot.

When the surface was scanned at -1 V and 1 nA we found that the deposited molecules on the Au {111} surface arranged themselves along the [1$\bar{1}$0] direction of herringbone in a zig-zag manner as shown in figure 5.3(a) to form supramolecular structure. Some of them are also randomly arranged around the step edges. The molecules are present at a slanting angle on the surface. From the arrangement it is clear that the molecules are standing on the surface on one of its sides. In between the molecules there exists some empty spaces which might be due to the drifting of some loose molecules while scanning the surface. The deposited molecules form a monolayer thick molecular layer (1ML) ~ 0.2 nm. Few molecules are loosely protruding from the surface (white circle) as shown in fig. 5.3(b). The further magnified image of the same layer is shown in fig. 5.3(c).

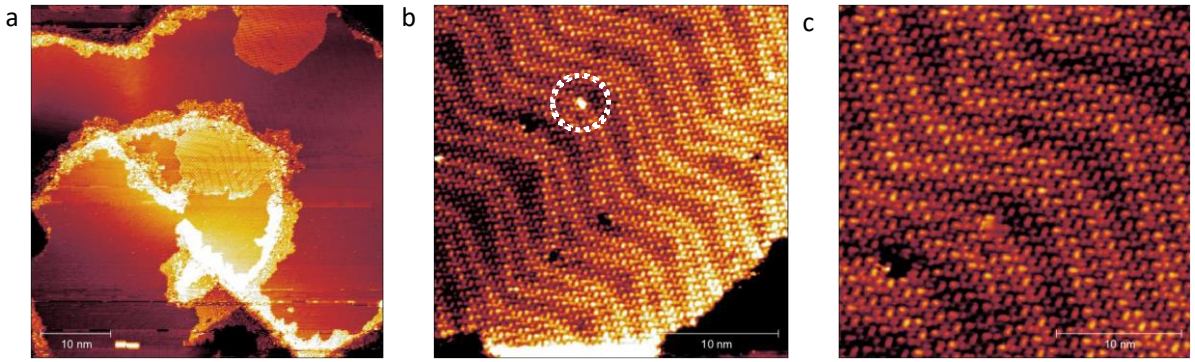

Fig. 5.3 (a) The Au (111) surface after the deposition of 1 monolayer thick DDQ molecule. The molecules are scattered at the edges but are arranged regularly to form a self-assembled structure at the middle of the Au surface. (b) The scanned area showing the self-assembled layer of the molecules. The white dotted circle shows a loose molecule on the surface laying flat. (c) The magnified image of the surface with clear arrangement of the molecules on the herringbone to form a zig-zag pattern for the self-assembled layer. The scale bar for the three images is 10 nm.

After the deposition of the molecules on the Au {111} surface they arranged themselves in multiple different ways. The one shown in fig. 5.4(a) is the one found statistically in a greater number of places on the surface. Fig. 5.4(b) shows arrangement of the molecules in some other place on the surface.

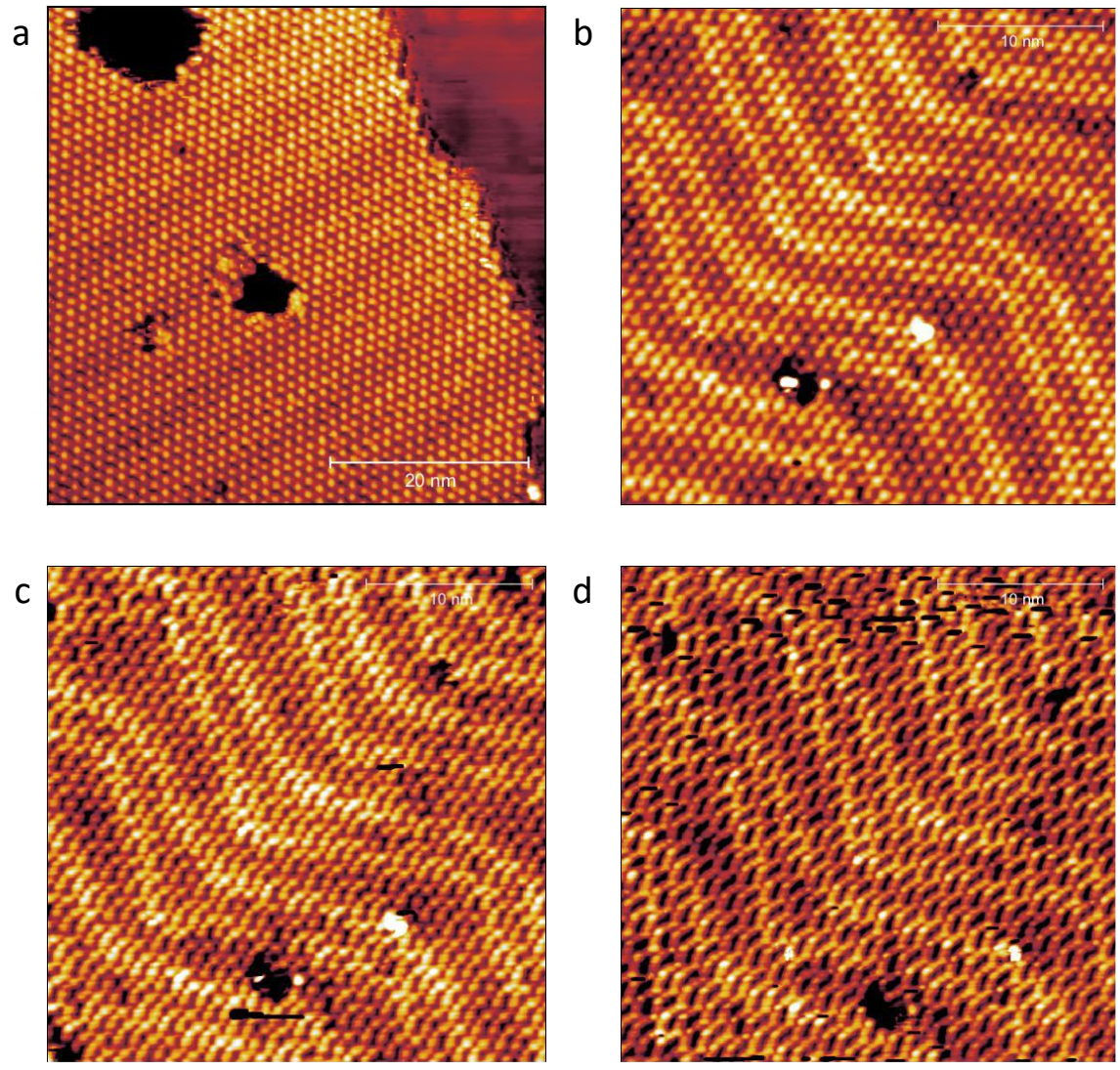

Fig. 5.4 (a) A uniformly self-assembled single layer of molecules on Au {111} surface which is the most favorable arrangement of the molecules on the surface. (b) Another arrangement of molecules which is found on the surface but least preferred. (c) and (d) The surface in image (b) is rotated at some angle about the z-axis to see the molecules from a different perspective.

This arrangement is least preferred configuration for the molecules as they are not widely present on the surface and hence may not be the most energetically favorable configuration. When the surface in fig. 5.4(b) is rotated about the z-axis by some angles the molecules' arrangement can be seen from a completely different perspective shown in fig. 5.4(c) and (d). The surface was scanned at different places and various types of orientation of the molecule was observed as shown in fig. 5.4. The one which is most widely found on the surface shown in fig. 5.4(a) was chosen as it must be the lowest energy configuration.

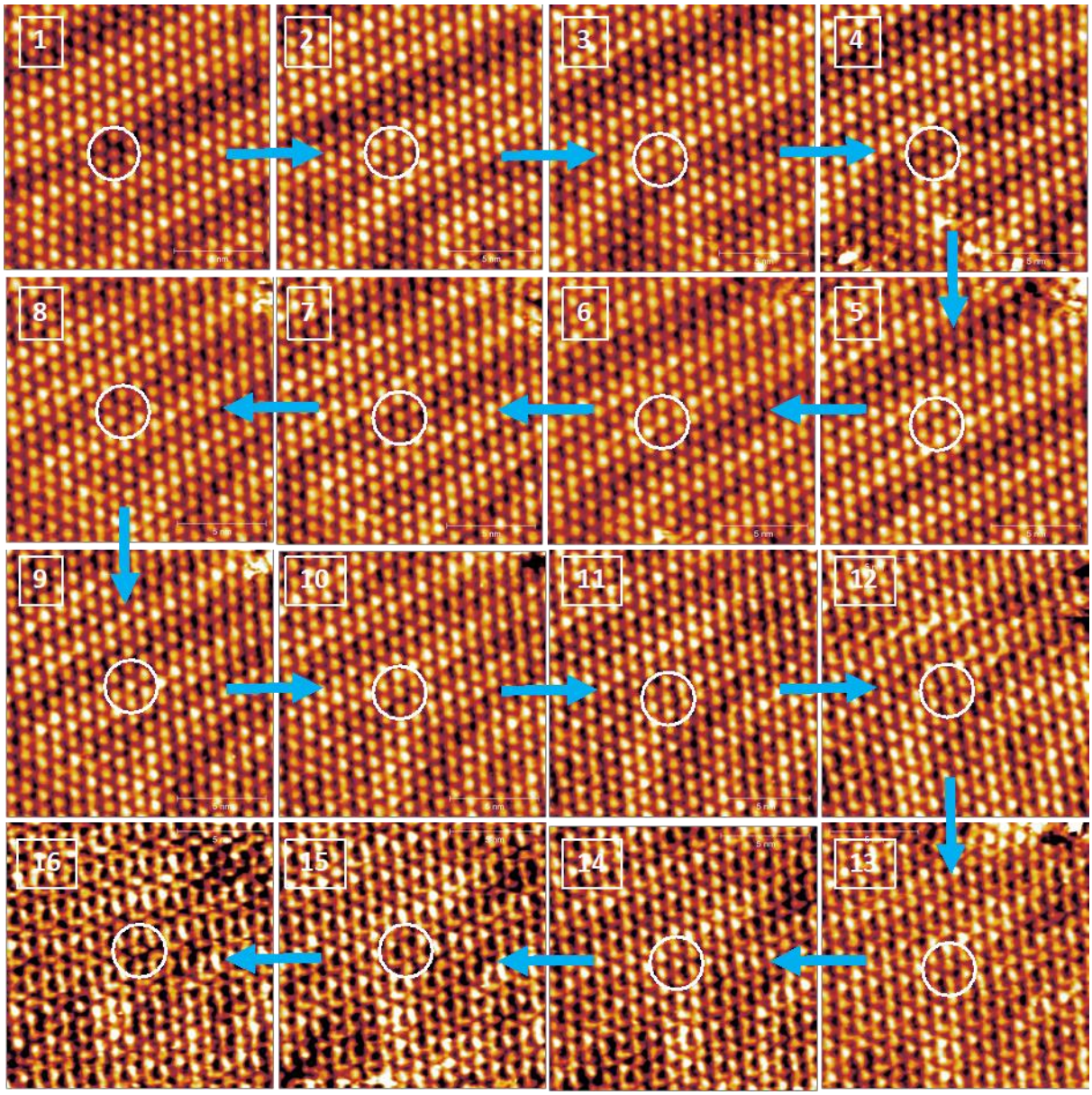

Fig. 5.5. Topographical images of DDQ deposited on Au {111} surface. Here each bright dot represents a DDQ molecule. These blocks numbered from 1 to 16 represent the image taken at voltages starting from -0.95 V to -0.2 V with a gap of 0.05 V. The blue arrows guide the direction of the decrement of voltage. The white circle represents the focused area of change under the applied bias. The scale bar in each represents 5 nm.

The DDQ deposited Au {111} substrate is scanned at a voltage of -0.95 V and is shown in the block 1 of fig. 5.5. As can be noticed that the molecules are present in a self-assembled manner

on the Au substrate and are mostly following the herringbone of the underneath Au surface as shown in fig. 5.5. So, this surface was scanned till there is zero thermal drift or creep of the surface to ensure the effects of applied voltage. We scanned the same area by varying the scan voltage from -0.95 V to -0.2 V with a voltage difference of 0.05 V. From the next block (block-2) onward instead of following the whole image we will focus only on the white circular area which contains seven DDQ molecules in it. A comparison of the two images in block 1 and 2 (scanned at -0.9 V) tells us that the contrast of the molecules in the circle has changed and they have become brighter in block 2 than block 1.

A close observation shows us a change in the spatial location as well. The position of the circle kept shifting with the decrease in the reverse voltage till block 10 but from block 11 (-0.45 V) onwards not only the position of the circle changed but also the orientation of the molecules inside the circle started changing. This can be verified by observing the change in the orbital configuration of one of the molecules on the top right part of the circle in the same block, which gives the impression that two molecules are fused. In the subsequent blocks, the orientation of other molecules also changes, which are distinct from the image of block 15 (-0.25 V) where more than one molecule has changed the configuration of the molecular orbital. In the end, for block 16 (-0.2 V) there is an entirely different orientation for all the molecules such that there is no similarity with block 1 (-0.95 V).

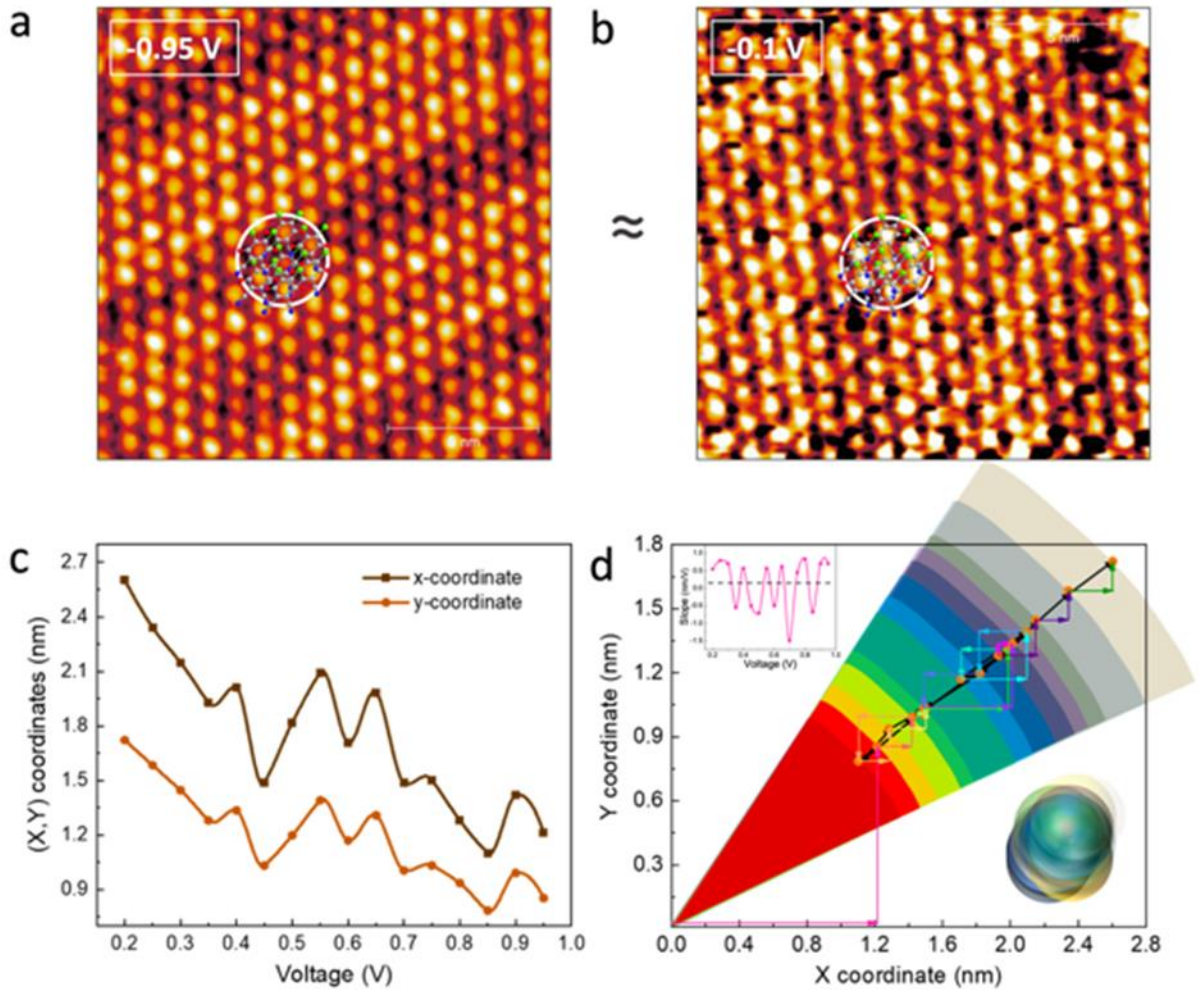

Fig. 5.6. The white circle in the topographic image has been tracked by using the coordinates (x,y) of a random point on the circumference of the circle. (a) The topographic image of the molecule scanned at -0.95 V. (b) The topographic image of the molecules scanned at -0.1 V. (c) The change in the coordinates of a particular point on the circumference with the applied scanned voltage (magnitude only). (d) The change in the x-coordinate with respect to the y-coordinate. The left top inset shows the change in slope with applied scanned voltage (magnitude only) after each movement, where the dotted line shows the average movement for the circle. The bottom right inset shows the overlapped image of all the circles giving a perspective on the phase change due to each movement.

At this point, the molecules are arranged in such a way that they formed a triangular honeycomb-like structure. It is found that after this block when the voltage decreased further down, it returned to the original position represented by the molecules of block 1 with identical coordinates but the image becomes better when we slightly increase the current by 0.05 nA which also gives us a hard-reset option. The scanned surface at -0.95 V and at -0.1 V are shown in fig. 3(a) and (b) for comparing the coordinates of both the molecular positions.

To follow the trail of the white circle in the topographic image discussed in the previous section, a random point on the circumference of the circle was chosen. This is the circle around the molecules scanned at -0.95 V. The coordinates (x, y) of this point was measured from the center of the circle. For the next scanned voltage (-0.9 V) the coordinates of the same shifted point from the center of the circle was measured, and in the same way, the shifted points in the subsequently scanned voltages till -0.2 V was measured and the change in these coordinates with applied scanned voltage is shown in fig. 5.6(c). As it can be seen that the change in position with scanned voltage is oscillatory, but one thing is evident that the coordinates are diverging from each other as well as from the initial position of the circle. The diverging resultant vector is 1.7 nm which is equivalent to the separation between two molecules.

To study the relationship between the x and the y coordinates, we observed their position with respect to each other, as shown in fig. 5.6(d). Here we have chosen each position with a proportional conic section to see the extent of the deviation. The x and y coordinates are shown by the vectors (different color arrows for different points) whose magnitudes are proportional to the amount of movement. The arrowhead position tells the direction of movement, the one showing to the right and up represents a positive movement, and the one showing to the left and down represents a negative movement. So the observed movement of this point from -0.95 V to -0.2 V shows that the motion is mostly in a straight line which tells that the bunch of molecules movement in the x,y plane is translational in nature. There is a very slight deviation from a straight line, but the deviation becomes apparent when we studied the change in the slope of each tangent with respect to the applied scanned voltage which is shown in the top left inset of fig. 5.6(d). It can be seen that the slope is oscillating around the average point shown by the dashed line. The bottom right inset of fig. 5.6(d) gives us a perspective of the change in phase with each movement of the point as it is obtained by overlapping all the filled colored circles one over the other and by tuning the transparency in such a way that one can see the bottom most filled circle as well.

To visualize the same thing from a new perspective, we tried to see the self-assembled molecules from a different orientation, and for that, we rotated the substrate by the z-axis at various angles and in both clockwise and counter-clockwise manner. The best orientation was obtained when rotated at an angle of 30˚ in a clockwise direction. The topographic images of the unrotated and rotated substrates are shown in fig. 5.7(a) and (b) respectively, and their corresponding schematic representations are shown in fig. 5.7(c) and (d). We have shown the same change in orientation of a single molecule in fig. 5.7(e). From fig. 5.7(b) we noticed that the molecules are arranged in a group of three nearby molecules (white rectangle) and a fourth molecule (green circle) is stranded close to the group of three molecules.

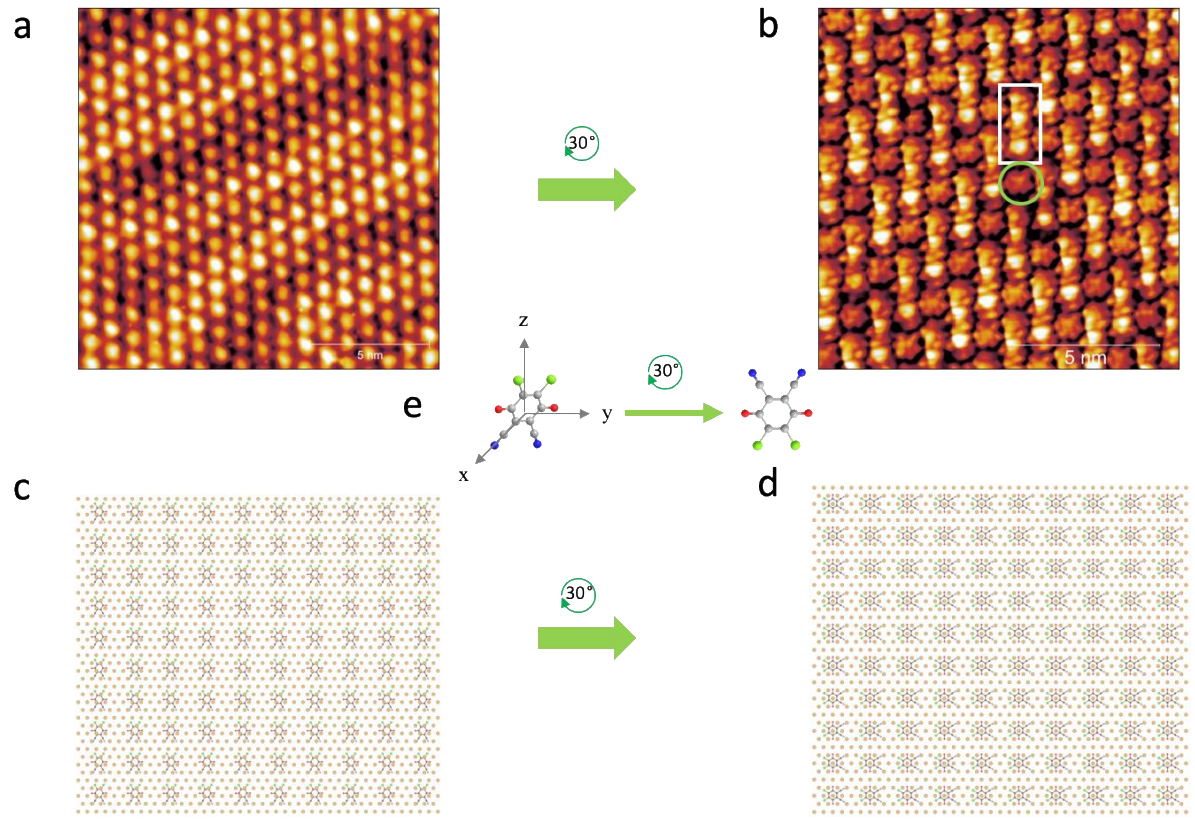

Fig. 5.7. The effect of rotation on the topographic image. (a) The topographic image obtained at a scan voltage of -0.95 V. (b) The same topographic image after 30˚ rotation in the clockwise direction by the z-axis. The white rectangle is a group of three molecules, and the green circle is a single molecule. (c) The simulated image of (a) with the most likely orientation of the molecules. (d) The simulated image of (b) with the most likely orientation of the molecules. (e) Schematic representation of the change in orientation of a single molecule after an anticlockwise rotation of 30˚ about the z-axis. The white line in the topographic images represents a length scale of 5 nm.

So, it can be perceived that such assemblies of four molecules are present all over the surface, and they constitute the bulk of the self-assembled structure. The detail arrangement of the molecules on the surface is shown in fig. 5.8. The difference in the orientation of the molecules in the two configurations is creating the illusion of a continuous arrangement of molecules in fig. 5.7(a) and a bundle of four molecules in fig. 5.7(b).

From STM images the length and width of the molecule was found to be 0.97 nm, and 0.69 nm respectively. The molecules are arranged in a fashion to form the interlock. From the fig. 5.8 one can see that as if the self-assembled structure is formed by considering the unit cell of a group of 3 bonded molecules (grey rectangles) and a relatively isolated molecule (blue circles). There are few areas where the three molecules are fused and in some other places the single molecule is relatively far apart. Four relatively separated molecules (blue circles) are present at the corners of a rectangle formed by the two vectors $\vec{a} = 1.01\, nm\, \hat{\jmath} + 1.36\, nm\, \hat{k}$ and $\vec{b} = 1.71\, nm\, \hat{\jmath} - 1.36\, nm\, \hat{k}$.

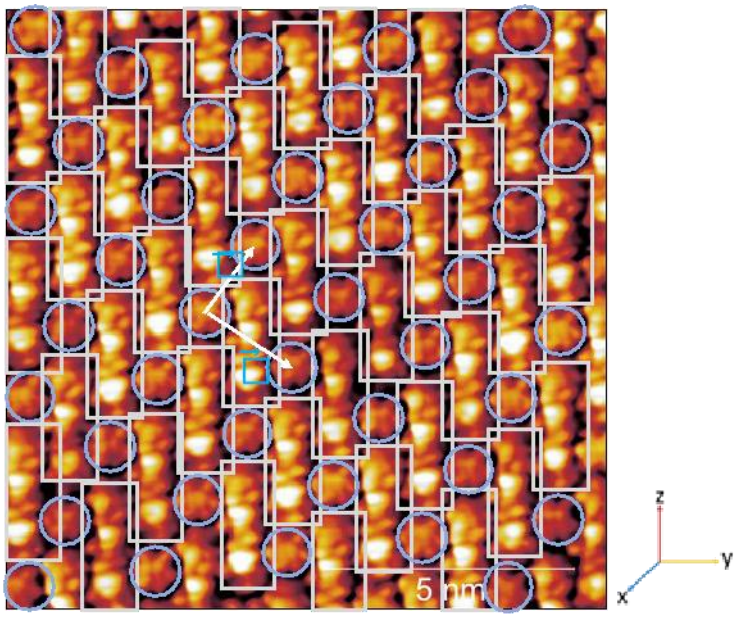

Fig. 5.8 The molecules which are rotated at an angle of 30° from its original position showed the planar structure of the molecule. The surface showed an arrangement of molecules where three molecules are almost strongly bonded (gray box filled with green color) with each other whereas the fourth molecule (blue circle filled with purple color) is relatively far apart from the other 3 molecules. The two-unit vectors are shown by the vectors $\vec{a}$ *and* $\vec{b}$. The scale bar is 5 nm and the x, y, and z coordinates are shown by blue, yellow, and red arrows.

A rectangle of the trimolecular structure which is encapsulated within the grey box filled with green color sandwiches two relatively isolated molecules (blue circle filled with purple color) and when the units are repeated, it formed the whole self-assembled structure on the surface.

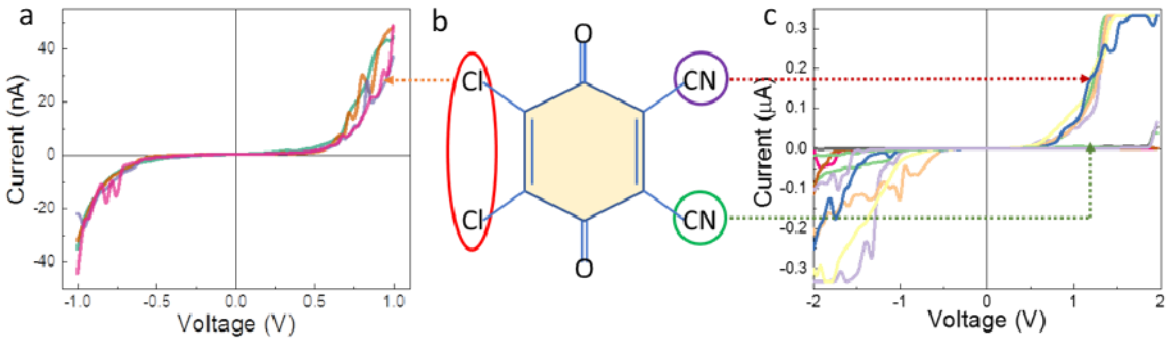

Fig. 5.9 (a) Four I-V characteristic curves obtained from the Cl ends (two from each Cl end) of the molecule within the voltage range of -1 to 1 V. The orange color dotted arrow from the red ellipse is pointing towards the I-V curves obtained from the Cl ends. The order of the current at 1 V is almost same for all the four curves and all of them show NDR effect in them. (b) The structure of the molecule with the red ellipse represents the two Cl end producing same current at a given bias. The green and the magenta circles represent the cyanide functional group ends of the molecule which give different orders of current in the output. (c) Two groups of I-V characteristic curves and each having four I-V curves from each CN end of the molecule. The I-V curves obtained from the top and bottom CN groups are shown by the red and green dotted lines respectively.

Before analyzing the group of molecules, we first probed each functional part of the molecule by taking the I-V curves from them. First the Chlorine (Cl) ends of the molecule are probed and it was found that the I-V curves show similar behavior having same orders of current as shown in fig. 5.9(a). Left hand side of the molecule marked by the red ellipse shown in fig. 5.9(b) corresponds to the area for recording the I-V characteristic from the Cl ends of the molecule. The two O ends of the molecule have also the same order of current. When the I-V curves from

each of the CN groups were studied it was found that there is orders of difference in the currents from both the groups as shown in fig. 5.9(c). The current (300 nA) from the top CN group (magenta circle) is one order higher than the current (50 nA) from the bottom CN group (green circle) shown in fig. 5.9(b). So, though both the functional groups are same, but it is perhaps the difference in orbital overlapping or the broken symmetry (Pati et al., 2008) of the phase of the molecule which is causing such change in the magnitude of the current. The current levels are much higher maybe because of the high electron localization in one of the CN groups.

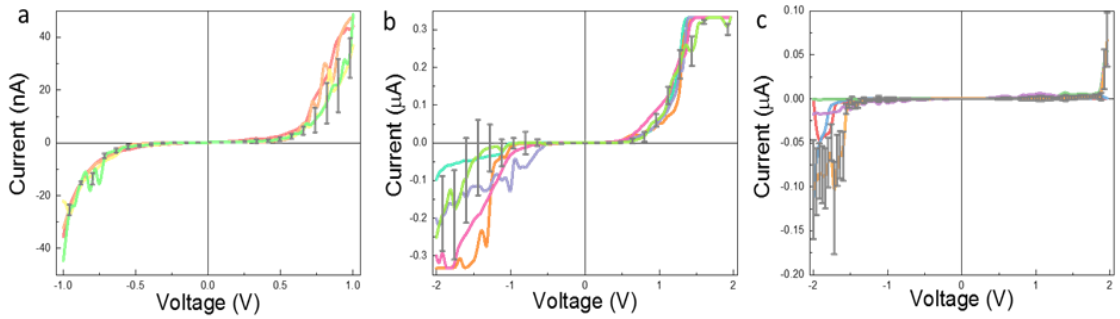

Fig. 5.10 (a) The I-V curves from the Cl functional group of the molecule scanned between -1 V to +1 V. The standard deviation for the I-V curves is also shown by using the error bars. (b) The I-V curves from the upper CN functional group of the molecule within the range of -2 to +2 V. Here also the standard deviation is shown by the error bars. (c) The I-V curves from the lower CN functional group of the molecule in the voltage range of -2 to +2 V. the two CN functional groups have one order difference in the current value.

Hundreds of I-V characteristic curves were taken from various parts of the molecule. The main parts of the molecule from which the I-V curves were recorded are the three functional groups such as Cl, O, and CN. The I-V from the Cl side of the molecule consistently gave same kind of I-V curves from both the Cl groups without much change in the behavior as well as the order of the current as seen in fig. 5.10(a). The error bars of the I-V data are also shown in the figure. Similarly, for the CN functional group the I-V curves for the upper and lower functional groups are different in terms of the order of current as shown in fig. 5.100(b) and (c). The error bars that we would like to highlight is for the positive side of the I-V curves as the variation in the magnitude and order of current is considered for the positive side.

Now the set of four molecules is studied further to understand the role they play in the translational motion of the molecules such that they eventually come back to the original position after a defined number of steps. In fig. 5.11(a) the four molecules are connected with each other as the orbital overlapping is visible from the figure. The orientation of the molecule can be understood by following the overlapped molecular structure. It turned out that the four molecules can be modeled as a series of four flip-flops forming a four-bit counter. The input to the flip-flops is given by the applied scanning potential through the O end of the molecule and since there is only one input end so we can consider the molecule to behave as a D flip-flop. The D flip-flop behavior was also ensured from fig. 5.10 because on one side its O ends give the same current output and can act as the D input. In the other side, the top CN group acts as the Q output and the lower CN group acts as the Q′ output.

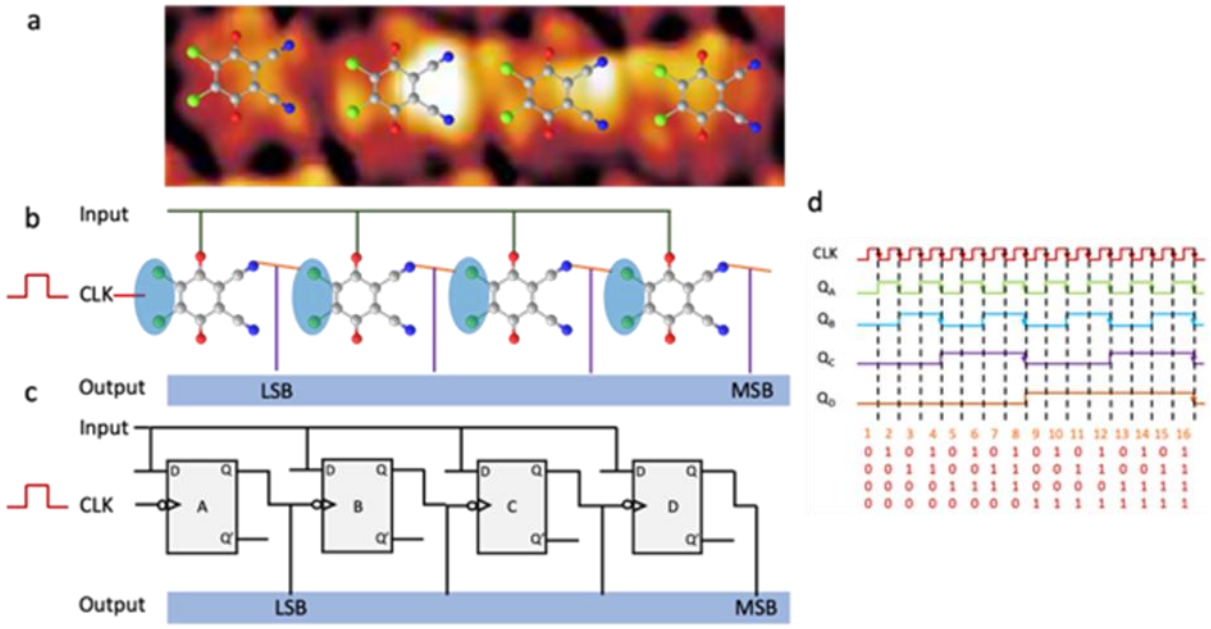

Fig. 5.11 (a) a small section of the rotated topographic image in which four molecules are connected to form a four-bit counter. The orientation of the molecule can be understood by looking at the overlapped stick and ball molecular structure. (b) A schematic of how the four-bit counter is formed by the four DDQ molecules. The input signal is given to the oxygen atoms. The orbital of the nitrogen atom of each molecule is overlapped with the orbital of the chlorine atom of the adjacent molecule. The output is obtained from the nitrogen atom end of the molecule. The clock signal is connected to the chlorine atoms. (c) a schematic of the digital representation of the four molecules as four flip-flops named as A, B, C, and D. Each flip-flop has one input and two (inverting (Q') and non-inverting (Q)) outputs. (d) The truth table of the counter with the four outputs from the four flip-flops along with the clock signal. The LSB and the MSB of the outputs are collected from the leftmost and the rightmost flip-flop in the series.

The surface is scanned at a constant scan raster time of 1ms per point for a 500x500 (points x lines) frame which performs as the clock signal, and this signal is acted at the Cl end of the molecule by its orientation. Since the clock signal is connected to both the chlorine atoms simultaneously, so we can think of them as only one end. This is shown by a blue ellipse over the two chlorine atoms in fig. 5.11(b). The output is collected from the non-inverting end (Q) of the flip-flop. The digital representation of the counter circuit is shown in fig. 5.11(c). From an n number of flip-flop based counter, it is known that the number of outputs is 2^n, since in our case there are four flip-flops, so the number of outputs is 16. The digital fingerprint of the outputs is shown by the timing diagram in fig. 5.11(d), where the output from the first flip-flop is following the clock signal and the output from the subsequent flip-flops is following the signal from the non-inverting end of the flip-flop. The digital representations of these 16 states are given from 0000 to 1111.

5.5 Analysis

The use of an asynchronous counter circuit to understand the perpetual translational motion of the DDQ molecules on the Au {111} surface leads to the idea that the circuit can be used for the conversion of analog to a digital signal (A/D) in the massive scale without using the conventional conversion methods. Due to asymmetry the DDQ molecule acts as a dipole and respond to the applied electric field. Here we have deposited one layer of DDQ molecules which have self-organized themselves on Au {111} surface via weak interaction. As we have shown (Sahu et al., 2012) that the DDQ molecule takes a prolate shape such that under applied field rotates about the central axis (z-axis) and since the molecule is oriented at 30° to the surface so the rotation causes movement of other molecule to create an iso-potential channel between the molecules. The rotational/translational motion is possible because the molecule we are using

inherently has redox behavior which responds to the change in the applied voltage, i.e., the molecule changes its conformation at some particular voltage where it can accept electrons and undergo reduction. DDQ molecule can reduce twice, once by accepting one electron and second by accepting another electron (Bandyopadhyay et al., 2010). This causes a change in the conformation of the molecule and hence a change in conductance of the molecule, one will be a high conducting state (logic state 1), and the other one is a low conducting state (logic state 0). Since the four molecules are connected one after another and each has two possible states (0, 1), a combination of 16 outputs can be possible, which is what is happening in the self-assembled layer. The DDQ and DDQ like molecules (DRQ) are known to interact with the neighboring molecules when the applied bias has changed; they are known to behave as molecular motors (Bandyopadhyay and Acharya, 2008) when they have sufficient degrees of freedom. They then form a supramolecular structure, and it has been shown that the whole supramolecular structure can be controlled by tuning the voltage to only one molecule, and the other molecules will follow the instructions. In our case also, the molecules are interacting with each other, but due to limited degrees of freedom, they have only restricted movement. The SET and RESET conditions of the counter are controlled by the movement of the molecules. The SET condition is defined by a set of particular coordinates of the molecule and once the counter started the coordinates of the molecules keep changing when a minimum step voltage of 0.05 V was applied between the tip and the molecule. The coordinates come back to the same initial state after 16 steps at which point the counter RESETs. A change in applied voltage means a shift in the position of the group of molecules, and that corresponds to a new digital signature. So here the counting is a process in which each new coordinate for the group of molecules take the counter forward/backward till the coordinates become exactly the same as that of the SET state. Since such assembly of four molecules is present all over the scanned area a change in voltage causes a consorted translation of the molecules globally over the whole surface but repeats itself after a few numbers of movements as in the local scale, it is controlled by a group of four molecules which forms a 4-bit asynchronous counter. So, we have tried to achieve the smallest possible 4-bit asynchronous counter useful for the conversion of the analog signal to a digital signal. Further research is undergoing on the effect of increasing the number of voltage steps on the counter circuit.

5.6 Conclusions

A 4-bit asynchronous counter has been achieved by using organic molecules, which have helped in the conversion of the analog signal to a digital signal. A change in position of the molecules represents the analog signal and is controlled by the 4-bit counter, and it resets the counter once the required number of steps is over. We can also hard reset the counter by changing the set current value. A corresponding digital signature will be assigned to each such new position. Though the change in position of the molecules is diverging it is happening linearly hence the motion is mostly translational in nature. Owing to the redox active nature of the molecule, the conductivity can be tuned by varying the applied potential. This leads to a change in conformation of the molecule and hence the orientation of the molecule. Since a group of four molecules are connected with each other, a change in the orientation of one molecule causes a change in the orientation of another molecule, i.e., by obeying the output of the preceding molecule except for the first molecule which will follow the clock signal and the input signal.